

accepted for publication in the Astrophysical Journal on Feb
20, 2012

High Resolution Images of Orbital Motion in the Orion Trapezium Cluster with the LBT AO System¹

Close, L.M.¹, Puglisi, A.², Males, J.R.¹, Arcidiacono, C.⁶, Skemer, A.¹, Guerra, J.C.³,
Busoni, L.², Brusa, G.³, Pinna, E.², Miller, D.L.³, Riccardi, A.², McCarthy, D.W.¹,
Xompero, M.¹, Kulesa, C.¹, Quiros-Pacheco, F.², Argomedo, J.², Brynnel, J.³, Esposito,
S.², Mannucci, F.², Boutsia, K.^{3,4}, Fini, L.², Thompson, D.J.³, Hill, J.M.³, Woodward,
C.E.⁵, Briguglio, R.², Rodigas, T.J.¹, Briguglio, R.², Stefanini, P.², Agapito, G.², Hinz, P.¹,
Follette, K.¹, Green, R.³

lclose@as.arizona.edu

¹*Steward Observatory, University of Arizona, Tucson, AZ 85721, USA*

²*INAF - Osservatorio Astrofisico di Arcetri, I-50125, Firenze, Italy*

³*LBT Observatory, University of Arizona, Tucson, AZ 85721, USA*

⁴*INAF-Osservatorio Astronomico di Roma, Via Frascati 33, I-00040, Monteporzio, Italy*

⁵*University of Minnesota Minneapolis, MN 55455 USA*

⁶*INAF - Osservatorio Astronomico di Bologna, I-40127 Bologna Italy*

ABSTRACT

The new 8.4m LBT adaptive secondary AO system, with its novel pyramid wavefront sensor, was used to produce very high Strehl ($\gtrsim 75\%$ at $2.16\mu m$) near infrared narrowband ($Br\gamma$: $2.16\mu m$ and $[FeII]$: $1.64\mu m$) images of 47 young (~ 1 Myr) Orion Trapezium θ^1 Ori cluster members. The inner $\sim 41 \times 53''$ of the

⁰¹The LBT is an international collaboration among institutions in the United States, Italy and Germany. LBT Corporation partners are: The University of Arizona on behalf of the Arizona university system; Istituto Nazionale di Astrofisica, Italy; LBT Beteiligungsgesellschaft, Germany, representing the Max-Planck Society, the Astrophysical Institute Potsdam, and Heidelberg University; The Ohio State University, and The Research Corporation, on behalf of The University of Notre Dame, University of Minnesota and University of Virginia.

cluster was imaged at spatial resolutions of $\sim 0.050''$ (at $1.64\mu m$). A combination of high spatial resolution and high S/N yielded relative binary positions to ~ 0.5 mas accuracies. Including previous speckle data, we analyze a 15 year baseline of high-resolution observations of this cluster. We are now sensitive to relative proper motions of just ~ 0.3 mas/yr (0.6 km/s at 450 pc) this is a $\sim 7\times$ improvement in orbital velocity accuracy compared to previous efforts. We now detect clear orbital motions in the θ^1 Ori B_2B_3 system of 4.9 ± 0.3 km/s and 7.2 ± 0.8 km/s in the θ^1 Ori A_1A_2 system (with correlations of PA vs. time at $> 99\%$ confidence). All five members of the θ^1 Ori B system appear likely as a gravitationally bound “mini-cluster”. The very lowest mass member of the θ^1 Ori B system (B_4 ; mass $\sim 0.2M_\odot$) has, for the first time, a clearly detected motion (at 4.3 ± 2.0 km/s; correlation=99.7%) w.r.t B_1 . However, B_4 is most likely in an long-term unstable (non-hierarchical) orbit and may “soon” be ejected from this “mini-cluster”. This “ejection” process could play a major role in the formation of low mass stars and brown dwarfs.

Subject headings: instrumentation: adaptive optics — binaries: general — stars: evolution — stars: formation — stars: low-mass, brown dwarfs

1. INTRODUCTION

The detailed formation of stars is still a poorly understood process. In particular, the formation mechanism of the lowest mass stars and brown dwarfs is uncertain. Detailed 3D (and N-body) simulations of star formation by Bate et al. (2002, 2003, 2009, 2011) and Parker et al. (2011) all suggest that stellar embryos frequently form into “mini-clusters” which dynamically decay, “ejecting” the lowest mass members. Such theories can explain why there are far more field brown dwarfs (BD) compared to BD companions of solar type stars (McCarthy & Zuckerman 2004) or early M stars (Hinz et al. 2002). Moreover, these theories which invoke some sort of dynamical decay (Durisen, Sterzik, & Pickett 2001) or ejection (Reipurth & Clarke 2001) suggest that there should be no wide (> 20 AU) very low mass (VLM; $M_{tot} < 0.185M_\odot$) binary systems observed in the field (age ~ 5 Gyr). Indeed, the AO surveys of Close et al. (2003a) and the HST surveys of Reid et al. (2001a); Burgasser et al. (2003); Bouy et al. (2003); Gizis et al. (2003) have not discovered more than a few wide (> 16 AU) VLM systems of the systems in the field population (for a review see Burgasser et al. (2007)). Additionally, the dynamical biasing towards the ejection of the lowest mass members naturally suggests that the frequency of field VLM binaries should be much lower ($\lesssim 5\%$ for $M_{tot} \sim 0.16M_\odot$) than for more massive binaries ($\sim 60\%$ for $M_{tot} \sim 1M_\odot$). Indeed,

observations suggest that the binarity of VLM systems with $M_{tot} \lesssim 0.185M_{\odot}$ is 10 – 15% (Close et al. 2003a; Burgasser et al. 2003, 2007) which, although higher than predicted is still lower than that of the $\sim 60\%$ of G star binaries Duquennoy & Mayor (1991). However as is noted in Close et al. (2007) there is evidence that in young clusters wide VLM binaries are much more common than in the old field population. They attribute this to observing these wide VLM systems before they are destroyed by encounters in their natal clusters. Hence, we need to look at nearby young clusters to see these low-mass objects before ejection has occurred.

Despite the success of these decay or ejection scenarios in predicting the observed properties of low mass VLM stars and binaries, it is still not clear that “mini-clusters” even exist in the early stages of star formation. To better understand whether such “mini-clusters” do exist we have examined the closest major OB star formation cluster for signs of such “mini-clusters”. Here we focus on the θ^1 Ori stars in the famous Orion Trapezium cluster. Trying to determine if some of the tight star groups in the Trapezium cluster are gravitationally bound is a first step to determining if bound “mini-clusters” exist. Also it is important to understand the true number of real, physical, binaries in this cluster, as there is evidence that the overall number of binaries is lower (at least for the lower mass members) in the dense trapezium cluster compared to the lower density young associations like Taurus-Auriga (McCaughrean 2000; Kohler et al. 2006). In particular, we will examine the case of the θ^1 Ori A and B groups in detail.

The Trapezium OB stars (θ^1 Ori A, B, C, D, and E) consists of the most massive OB stars located at the center of the Orion Nebula star formation cluster (for a review see Genzel & Stutzki (1989)). Due to the nearby and luminous nature of these stars they have been the target of several high-resolution imaging studies. Utilizing only tip-tilt compensation McCaughrean & Stauffer (1994) mapped the region at K' from the 3.5-m Calar Alto telescope. They noted that θ^1 Ori B was really composed of 2 components (B_1 & B_2) about $\sim 1''$ apart. Higher $\sim 0.15''$ resolutions were obtained from the same telescope by Petr et al. (1998) with speckle holographic observations. At these higher resolutions Petr et al. (1998) discovered that θ^1 Ori B_2 was really itself a $0.1''$ system (B_2 & B_3) and that θ^1 Ori A was really a $\sim 0.2''$ binary (A_1 & A_2). A large AO survey of the inner 6 square arcminutes was carried out by Simon, Close, & Beck (1999), who discovered a very faint (100 times fainter than B_1) object (B_4) located just $0.6''$ between B_1 and B_2 . Moreover, a spectroscopic survey (Abt, Wang, & Cardona 1991) showed that B_1 was really an eclipsing spectroscopic binary (B_1 & B_5 ; sep. 0.13 AU; period 6.47 days). As well, θ^1 Ori A_1 was also found to be a spectroscopic binary (A_1 & A_3 ; sep. 1 AU; Bossi et al. (1989)). Weigelt et al. (1999) carried out bispectrum speckle interferometric observations at the larger Russian SAO 6-m telescope (2 runs in 1997 and 1998). These observations showed θ^1 Ori C was a very tight $0.033''$ binary.

These observations also provided the first set of accurate relative positions for these stars. Schertl et al. (2003) has continued to monitor this cluster of stars and detected an orbital motion (of $\Delta PA \sim 6^\circ$ for θ^1 Ori A_2 around A_1 and a ΔPA of $\sim 8^\circ$ for θ^1 Ori B_3 around B_2 over a 5.5 yr baseline).

Close et al. (2003c) utilized the Gemini telescope (with the Hokupa’a AO system) and then observed θ^1 Ori B during commissioning of the first adaptive secondary deformable mirror at the 6.5-m MMT telescope. This extended the baseline by 2 years. Now during the science verification of the world’s first “next generation” adaptive secondary mirror with the LBT AO System the full Trapezium cluster was observed again with excellent performance (K Strehl $\gtrsim 75\%$). Now we have over 14 years of observations of this field with at $< 0.08''$ resolutions.

In this paper we outline how these LBT observations were carried out with the relatively new PISCES camera and LBT AO system (FLAO). We detail how these data were calibrated and reduced and how the stellar positions were measured. We fit the observed positions to calculate velocities (or upper limits) for the θ^1 Ori B & A stars. While Schertl et al. (2003) and Close et al. (2003c) had hints that the θ^1 Ori B group may be a bound “mini-cluster” —we show it is clearly so, with the first detection of orbital motion of the lowest mass member.

2. INSTRUMENTAL SET-UP

We utilized the LBT adaptive secondary AO system to obtain the most recent highest-resolution (unsaturated) images of the young stars in the Trapezium cluster (the θ^1 Ori group). This is not a simple task, since as telescopes have increased in size and (with AO) Strehl, so now the bright stars tend to saturate—in even the shortest exposures. Hence, special precautions are needed to avoid saturation of the bright Trapezium stars themselves. It is now almost impossible to make unsaturated, but diffraction-limited, images of the bright Trapezium stars with modern 8m class AO systems at high Strehl. Witness the fact that this is the first such dataset published in 9 years. Hence this dataset is unusually important. The next subsections outline how this was accomplished.

2.1. The LBT AO System

The 8.4m LBT telescope has a unique “first light adaptive optics” (FLAO) system. To reduce the aberrations caused by atmospheric turbulence all AO systems have a deformable

mirror which is updated in shape at ~ 500 Hz. Except for the MMTAO system (Wildi et al. 2003a; Hinz et al. 2010), all adaptive optics systems have located this deformable mirror (DM) at a re-imaged pupil (effectively a compressed image of the primary mirror). To reimage the pupil onto a DM typically requires 6-8 warm additional optical surfaces, which significantly increases the thermal background and decreases the optical throughput of the system (Lloyd-Hart 2000). However, the LBT utilizes a next generation adaptive secondary DM. This DM is both the secondary mirror of the telescope and the DM of the AO system (like with MMTAO). In this manner there are no additional optics required in front of the science camera. Hence the emissivity is lower. The LBT’s DM is a much more advanced “second generation” adaptive secondary mirror (ASM), which enables the highest on-sky Strehl ($> 80\%$ at H band) of any 8-10m telescope today (Esposito et al. 2011).

The LBT ASM consists of 672 voice coil actuators that push (or pull) on 672 small magnets glued to the backsurface of a thin (1.6 mm), 0.911 m aspheric ellipsoidal Zerodur glass “shell” (for a detailed review of the secondary mirror see Esposito et al. (2010a, 2011)). We have complete positional control of the surface of this reflective shell by use of a 70kHz capacitive sensor feedback loop. This positional feedback loop allows one to position an actuator of the shell to within ~ 5 nm rms (total wavefront surface errors amount to only ~ 50 nm rms over the whole secondary). The AO system samples (and drives the ASM) at 990 Hz using 400 active controlled modes (with 672 actuators) on bright stars ($R_i 8$ mag).

The wavefront slopes are measured with the very accurate (and well calibrated, with low aliasing error) Pyramid Wavefront sensor (PWFS). This is the first large telescope to use a PWFS. The performance of the FLAO PWFS is excellent. The uniquely low residual wavefront errors obtained by the PWFS + ASM combination is due, in part, to the very accurate (high S/N) interaction matrix that can be obtained in closed-loop daytime calibrations with a retro-reflecting optic that takes advantage of the Gregorian (concave) nature of the secondary. To guarantee strict “on-sky” compliance with the “daytime calibrated” interaction matrix pupil/ASM/PWFS geometry the PWFS utilizes a novel “closed-loop pupil alignment system” that maintains the pupil alignment to $< 2.5\mu\text{m}$ during all closed-loop operations on bright stars (like our Trapezium guide stars). For a detailed review of the LBT FLAO AO system see Esposito et al. (2011) and references within.

2.2. The LBT AO Observations

During LBT science verification (the last AO commissioning run of the first LBT ASM) we observed the θ^1 Ori B and C fields on the night of Oct 16, 2011 (UT). The AO system corrected the lowest 400 system modes and was updated at 990 Hz. Without AO correction

our images had FWHM= $\sim 0.5''$ at [FeII], after AO correction our final 10 min image achieved FWHM= $0.050''$ (close to the diffraction limit of $0.041''$ at [FeII] ($1.644 \mu m$)).

2.3. The PISCES NIR Camera

These observations utilized the first light AO science camera, PISCES, which has been modified for the LBT AO system. PISCES has a 1024×1024 $1\text{--}2.5 \mu m$ HAWAII array. Here we used the narrowband $Br\gamma$ ($2.16 \mu m$) and [FeII] ($1.644 \mu m$) filters to minimize saturation on the array. We also utilized a warm 25 mm dia. neutral density filter (ND2: with 1% transmission) which was custom mounted by flexible adhesive strips on the PISCES dewar within a few mm of the $f/15$ focal plane of the ASM. Since the high quality flat ND2 was nearly in the warm first focal plane (in front of the PISCES dewar window) it cannot significantly alter, or distort, the platescale or optical quality of PISCES.

The PISCES focal plane platescales were calibrated by the astrometry of seven single (relatively faint) stars ² from $3.4 - 8.5''$ from θ^1 Ori C (see sections 3 and 4 for more details about how the images were first distortion corrected and combined etc.). We note here that we only used the data where θ^1 Ori C was the guide star for the platescale calibration. The 3 dither frames that used this guide star were all taken within 20 min of each other, and so the PA angle is assumed to be fixed for all exposures.

The positions (found by IRAF *allstar* PSF fitting) of these seven stars from our LBT AO images were compared to unsaturated HST ACS WCS astrometry from the publicly available archived data of Ricci et al. (2007). Platescales and rms errors were then determined for the $Br\gamma$ and [FeII] filters with the IRAF *geomap* task. The *geomap* task found $0.019350 \pm 0.000047''/\text{pix}$ $Br\gamma$ platescale (providing a $19.8 \times 19.8''$ FOV). At [FeII] the platescale was slightly finer at $0.019274 \pm 0.000036''/\text{pix}$. For PISCES it is well known that, due to a slight focus change, the bluer wavelengths have a slightly finer platescale.

The steps used to align the Y axis of the PISCES images (which were all taken with the rotator following) it was first necessary to flip the image about the X axis. Then each image was rotated (with the IRAF *rotate* task) by the fixed PA+90 of the rotator (POSANGLE FITS keyword value +90 degrees). All 3 rotated images were then combined. At this point it was found by *geomap* in the $Br\gamma$ image that the direction of North was slightly (0.898°)

²Typically the stars in the Trapezium used for this platescale test move at only $\sim 0.0015''/\text{yr}$ so the platescale error over a $5''$ distance is $\sim 2 \times 10^{-5}\%$ error — which is much smaller than the rms fitting platescale errors of $\sim 0.25\%$.

East of PISCES’s Y axis compared to the HST image. Hence a final rotation of -0.898° was applied to the final image. At [FeII] this additional rotation was a very similar -0.959° value. The rms uncertainty adopted for the LBT rotator angle is estimated as $\sim 0.3^\circ$ which dominates the small 0.062° error between the two geomap solutions. We conclude that most of the $\sim 0.3^\circ$ is due to systematic errors in the distortion corrections.

The camera was mounted under a high optical quality dichroic which sent the visible light ($0.5\text{--}1\ \mu\text{m}$) to the 30×30 subaperture Pyramid wavefront sensor (PWFS; Esposito et al. (2010b)). The PWFS communicates with the the ASM mirror (which has 672 actuators, but ~ 20 were not operational on this run, with no real loss in performance). The infrared light ($\lambda > 1\ \mu\text{m}$) was transmitted through the dichroic to PISCES.

3. OBSERVATIONS & REDUCTIONS

For the θ^1 Ori C field we locked the AO system (at 990Hz, 400 modes) on the bright O5pv star θ^1 Ori C ($V=5.13$ mag) and dithered over 3 positions on the PISCES array with a short set of 10×0.8 second unsaturated exposures (save C1 which at $H=4.48$ saturated even in [FeII] with the ND2). Immediately following the unsaturated exposures a set of 10×20 second exposures were obtained at each dither position. This whole procedure was repeated with in $Br\gamma$ with slightly different dithers. Hence for a few sources on the edges of the frames there is only photometry in one filter. However, when reduced both filter images covered an area of $\sim 31 \times 24''$ centered on θ^1 Ori C. We note that θ^1 Ori C is really a $\sim 0.04''$ binary composed of C1 and C2, (see Kraus et al. (2007) for more details). Due to the very red nature of the Trapezium sources we only needed half the number of images at $Br\gamma$ compared to [FeII]. Hence we obtained $3\times 5\times 0.8$ second unsaturated exposures and $3\times 5\times 20$ second deeper exposures at $Br\gamma$.

Then the AO system was locked on the nearby star θ^1 Ori B1 ($V=7.96$ mag) and was dithered over a similar sized area to produce a set of $3\times 10\times 0.8$ s unsaturated images [FeII] images followed by $3\times 10\times 20$ s deeper images at [FeII]. Again half that data was obtained at $Br\gamma$ ($3\times 5\times 0.8$ s and $3\times 5\times 20$ s). The final image in the θ^1 Ori B field spanned $\sim 31 \times 24''$ centered on θ^1 Ori B1.

Before the images were combined each image was first corrected with PISCES appropriate values for the *corquad* “overshoot” program ³. Then they were distortion “pincushion”

³<http://aries.as.arizona.edu/~observer/dot.corquad.pisces>

corrected with the cubic distortion solution for PISCES from a pinhole array mask⁴ and the IRAF *drizzle* task. At this point the individual frames could be reduced in a normal manner. We used our custom AO image reduction script of Close et al. (2003a) to flat field, sky subtract, cross-correlate, and median combine each image. The final deep images of the C and B fields had a total exposure time of 10 min in the overlap region in the [FeII] images and 5 min in the $Br\gamma$ images. The unsaturated images had total exposure times of 24 s and 12 s in [FeII] and $Br\gamma$ respectively. Each of these reduced images were then flipped in X, rotated by POSANGLE+90 degrees, and corrected by -0.9 degrees –as described above to match the HST ACS astrometry with *geomap* to that of Ricci et al. (2007). Hence North is up and East is to the left in each of the final images.

While all astrometry and photometry was performed on these individual fields (on unsaturated images), the last step was combining these two C and B fields into a single large image of the entire Trapezium. The final images (see Figs. 1 and 2) have a size of $\sim 41 \times 53''$. This image is the largest AO image obtained by the LBT to date.

4. ASTROMETRY & PHOTOMETRY

All eight reduced images (the C and B fields at both [FeII] and $Br\gamma$ at both long and short exposures) were analyzed with the DAOPHOT PSF fitting task *allstar* (Stetson 1987). The photometry and astrometry are summarized in Table 1. The columns of Table 1 are self explanatory. We note that the zeropoints for the [FeII] and $Br\gamma$ photometry were arbitrary as these are narrow band filters. However, it is clear that the Δ magnitudes at [FeII] seem to closely track the true ΔH magnitudes, since these sources are mainly continuum at $1.64\mu m$. However, these sources are all accreting and have excess emission at $Br\gamma$. Hence, the [FeII]- $Br\gamma$ color given in the last column of Table 1 is largest for objects that have very active accretion and/or a high level of circumstellar absorption.

Note in the the deep $Br\gamma$ image, well known “tails” of emission point away from θ^1 Ori C, and are highlighted by blue rectangles in Fig. 3 and in the comments column of Table 1. Also each tight binary is called out in the table as well as each member of the bright Trapezium stars themselves. All the tight ($< 0.5''$) binaries have additional details in Table 3.

We minimized the small anisoplanatic PSF radial fitting errors in table 1 by using a spatially variable PSF in the DAOPHOT *psf* task. The most heavily weighted PSF star used

⁴<http://wiki.lbto.arizona.edu/twiki/pub/AdaptiveOptics/PiscesDistorsion/pisces.cubic>

was unsaturated θ^1 Ori B_1 itself. Since all the members of the θ^1 Ori B group are located within $1''$ of θ^1 Ori B_1 the PSF fit is particularly excellent there (there is no detectable change in PSF morphology due to anisoplanatic effects inside the θ^1 Ori B group (Diolaiti et al. 2000)). Moreover, the residuals over the whole field were less than a few % after PSF subtraction. This is not really surprising given the quality of the night combined with the fact that no star was further than $\sim 8''$ from the guide star. However, to minimize this affect, we only used the longer wavelength $Br\gamma$ astrometry in Table 1 where anisoplanatic PSF effects were much less significant.

The relative positional accuracy is an excellent ~ 0.5 mas for the bright binaries that are tighter than $0.2''$, but the absolute RA and DEC positions given in Table 1 are typically only good to $\lesssim 0.1''$ due to the 0.25% uncertainty in the platescale for this new instrument.

We can also compare our LBT data to older (somewhat less accurate) images of the Trapezium B stars from Close et al. (2003c) who used AO images from Gemini and the 6.5m MMT and speckle images from the literature (Schertl et al. 2003). Even though these individual observations are of lower quality and Strehl than the LBT ones (compare Figs. 4 and 5 to that of the LBT in Fig. 6), the 15 years between these observations and those of the LBT can highlight even very small orbital motions of bound systems in the Trapezium. It also shows the very significant improvement in high Strehl AO now possible with Pyramid wavefront sensors and next generation adaptive secondary mirrors (ASMs).

A test to see how accurate our astrometry is over the last 15 years is to look at the separation and PA of B_1 vs. B_2 . The scatter of the θ^1 Ori B_1B_2 separation (which should be very close to a constant since the B_1B_2 system has an orbital period of $\gtrsim 4000$ yr) will highlight systematic errors. The lack of any motion between B_1 and B_2 is also confirmed by Schertl et al. (2003) and Close et al. (2003c). Our detailed LBT and past data on the B and A groups from the literature is summarized in Table 2. Linear (weighted) fits to the data in Table 2 (Figures 7 to 14) yield the velocities shown in Table 2. The overall error in the relative proper motions observed is now $\lesssim 0.5$ mas/yr in proper motion ($\lesssim 1$ km/s).

5. ANALYSIS & DISCUSSION

With these accuracies it is now possible to determine whether these stars in the θ^1 Ori B group are bound together, or merely chance projections in this very crowded region. We adopt the masses of each star from the Siess Forestini & Dougados (1997); Bernasconi & Maeder (1996) tracks fit by Weigelt et al. (1999) where we find masses of: $B_1 \sim 7M_\odot$; $B_2 \sim 3M_\odot$; $B_3 \sim 2.5M_\odot$; $B_4 \sim 0.2M_\odot$; $B_5 \sim 7M_\odot$; $A_1 \sim 20M_\odot$; $A_2 \sim 4M_\odot$; and $A_3 \sim 2.6M_\odot$. Based on

these masses (which are similar to those adopted by Schertl et al. (2003)) we can comment on whether the observed motions are less than the escape velocities expected for simple face-on circular orbits.

Our combination of high spatial resolution and high signal to noise shows that there is no detectable motion in the B_1B_2 system over the last 15 years (as we would expect if the true separation is $\gtrsim 900$ AU). But we have observed clear orbital motion (at 4.9 ± 0.3 km/s) in the very tight θ^1 Ori B_2B_3 system in PA (see Figure 10). Also we see clear orbital motion (consistent with curvature) of 7.2 ± 0.8 km/s in the θ^1 Ori A_1A_2 system (see Figs. 11 and 12). We know this is likely orbital motion since both binaries have moved in an nearly circular arc of $\Delta PA \sim 15^\circ$ over the last 15 years with almost no change in the separation between components, hence it appears (at least with the limited amount of observed orbital phase) that both of these binaries are consistent with roughly circular, close to face-on, orbits.

5.1. Is the θ^1 Ori B_2B_3 System Physical?

The relative velocity in the θ^1 Ori B_2B_3 system (in the plane of the sky) is now more accurate by $\sim 7\times$ compared to that of Close et al. (2003c). Our new velocity of 4.9 ± 0.3 km/s is consistent, but with much lower errors, with the $\sim 4.2 \pm 2.1$ km/s of Close et al. (2003c) (this velocity is in the azimuthal direction; see Figure 10). This is a reasonable V_{tan} since an orbital velocity of ~ 6.7 km/s is expected from a face-on circular orbit from a $\sim 5.5M_\odot$ binary system like θ^1 Ori B_2B_3 with a 51 AU projected separation (implying an orbital period of order ~ 200 yr). It is worth noting that this velocity is also greater than the ~ 3 km/s Hillenbrand & Hartmann (1998) dispersion velocity of the cluster. Hence it is most likely that these two $K' = 7.6$ and $K' = 8.6$ stars (separated by just $0.115''$) are indeed in orbit around each other. Moreover, there are only 10 stars known to have $K' < 8.6$ in the inner $30 \times 30''$ (see Figure 2), we can estimate that the chances of finding two bright ($K' < 8.6$) stars within $0.115''$ is a small $< 10^{-4}$ probability.

Our observed velocity of $1.15 \pm 0.07^\circ/\text{yr}$ is consistent (in both direction and magnitude) with the $1.4^\circ/\text{yr}$ observed by Schertl et al. (2003) and the $0.93 \pm 0.49^\circ/\text{yr}$ of Close et al. (2003c). This suggests that the AO and speckle datasets are both detecting real motion, but the addition of the LBT dataset has reduced the errors by $\sim 7\times$. Moreover, since this motion is primarily azimuthal strongly suggests an orbital arc of B_3 orbiting B_2 .

5.2. Is the θ^1 Ori A_1A_2 System Physical?

We observe 7.2 ± 0.8 km/s of relative motion in the θ^1 Ori A_1A_2 system (mainly in the azimuthal direction; see Figure 12). This is higher than the average dispersion velocity of ~ 3 km/s yet well below an estimated escape velocity of the $\sim 20M_\odot$ A_1A_2 system (projected separation of 94 AU). Hence it is highly likely that these two $K' = 6.0$ and $K' = 7.6$ stars (separated by just $0.193''$) are indeed in orbit around each other. In addition, there are only 8 stars known to have $K' < 7.6$ in the inner $30 \times 30''$ (see Figure 2), we can estimate that the chances of finding two bright ($K' < 8.6$) stars within $0.19''$ is a small $< 4 \times 10^{-4}$ probability.

Our observed velocity of 7.2 ± 0.8 km/s is much more accurate (and lower) than the 16.5 ± 5.7 km/s found by Close et al. (2003c). Our new value is consistent (in both direction and magnitude) with the ~ 10.3 km/s observed by Schertl et al. (2003). This again suggests that the AO and speckle datasets are both detecting real motion of A_2 orbiting A_1 .

5.3. Is the θ^1 Ori B Group Stable?

The pair B_1B_5 is moving at a low $\lesssim 1$ km/s in the plane of the sky w.r.t. to the pair B_2B_3 where the escape velocity $V_{\text{esc}} \sim 6$ km/s for this system. Hence these pairs are very likely gravitationally bound together. However, radial velocity measurements will be required to be absolutely sure that these 2 pairs are truly bound together.

5.3.1. Is the Orbit of θ^1 Ori B_4 Stable?

The situation is somewhat different for the faintest component of the group, B_4 . It has $K = 11.66$ mag which according to Hillenbrand & Carpenter (2000) suggests a mass of only $\sim 0.2M_\odot$. Since there are only 20 stars known to have $K < 11.66$ in the inner $30''$ (see Fig. 6), we can estimate that the chances of finding a $K < 11.66$ star within $0.6''$ of B_1 is a small $< 8 \times 10^{-3}$ probability. The two AO measurements of Close et al. (2003c) (and the one speckle detection of Schertl et al. (2003)) did not detect a significant velocity of B_4 w.r.t. B_1 : 2 ± 11 km/s.

However, our much better data and timeline has shed some light on the question of B_4 orbiting B_1 . As is clear from Figures 13 & 14, there appears to be a real velocity of 4.3 ± 2.0 km/s detected. This is greater than the random velocity of the cluster yet below the escape velocity of ~ 6 km/s, this points towards B_4 being a gravitationally bound member of the θ^1 Ori B group. This is the first time we can say that the lowest mass member of the

B group is likely bound.

On the other hand, its very low mass and its projected location w.r.t. to the other four groups members makes it highly unlikely that B_4 is on a long-term stable orbit within the group. As we will discuss in the next section even the much more massive B_3 may not be stable in the long-term.

5.3.2. *Is the orbit of B_3 around B_2 and of B_5 around B_1 stable in the long-term?*

B_1B_5 , and B_2B_3 are two binaries with projected separations of 0.13 AU (B_1B_5) and 52 AU (B_2B_3); respectively. The two pairs are separated by a projected distance of 415 AU. The distance $D_{B_1B_5} \sim 3 \times 10^{-4} \times D_{B_1B_5B_2B_3}$ and thus the B_1B_5 system is stable. Much more interesting is the case of B_2B_3 . Their projected distance is not very small compared to their projected distance (D) from the B_1B_5 pair: $D_{B_2B_3} \sim 0.12 \times D_{B_1B_5B_2B_3}$. Thus the stability of the B_2B_3 orbit needs a more detailed analysis since it is possible that B_3 may be ejected in the future.

Eggleston & Kiseleva (1995) have given an empirical criterion for the long-term stability of the orbits of hierarchical triple systems, based on the results of their extensive model calculations (Kiseleva & Eggleston 1994; Kiseleva et al. 1994; Eggleston & Kiseleva 1995). Their analytic stability criterion is good to about $\pm 20\%$, and is meant to indicate stability for another 10^2 orbits. Given the uncertainties of the masses of the members of the B group, this accuracy is sufficient for our present discussion.

The orbital period of the two binaries w.r.t. each other is $P_{(15)/(23)} \sim 1920$ yrs, while the orbital period of B_3 w.r.t B_2 amounts to $P_{2/3} \sim 160$ yrs. For the calculation of both periods, we have assumed the masses as given above, and circular orbits in the plane of the sky. This leads to a period ratio $X = P_{(15)/(23)}/P_{2/3} \sim 12$. Eggleston & Kiseleva’s stability criterion requires $X \geq X_{crit} = 10.08$ for the masses in the B group. This means that within the accuracy limits of our investigation, the binary B_2B_3 is just at the limit of stability. The stability criterion depends also on the orbits’ eccentricities. In our case, already mild eccentricities of the order of $e \sim 0.1$ (as can be expected to develop in hierarchical triple systems; see, e.g., Georgakarakos 2002), make the B group unstable. While we cannot decide yet whether the pair B_2B_3 orbit each other in a stable way, it is safe to say that the “triple” B_1B_5 , B_2 , and B_3 is not a simple, stable hierarchical triple system.

The θ^1 Ori B system seems to be a good example of a highly dynamic star formation “mini-cluster” which might in the future eject the lowest-mass member(s) through dynamical decay (Durisen, Sterzik, & Pickett 2001), and breaking up the gravitational binding of the

widest of the close binaries (the B_2B_3 system). The "ejection" of the lowest-mass member of a formation "mini-cluster" could play a major role in the formation of low mass stars and brown dwarfs (Reid et al. 2001a; Bate et al. 2002; Durisen, Sterzik, & Pickett 2001; Close et al. 2003a). The breaking up of binaries, of course, modifies the binary fraction of main sequence stars considerably as well.

6. FUTURE OBSERVATIONS

Future observations are required to see, if indeed, these stars continue to follow orbital arcs around each other proving that they are interacting with one another. In addition, future observations of the θ^1 Ori B_4 positions would help deduce if it is on a marginally stable orbit given its "non-hierarchical" location in the B group.

Future observations should also try to determine the radial velocities of these stars. Once radial velocities are known one can calculate the full space velocities of these stars. Such observations will require both very high spatial and spectral resolutions. This might be possible with such instruments like the AO fed ARIES echelle instrument at the MMT.

We thank the anonymous referee for their helpful review of this paper. The authors thank Piero Salinari for his insight, leadership and persistence which made the development of the LBT adaptive secondaries possible. We thank the whole LBT community for making this wonderful telescope possible. LMC is supported by an NSF AAG and NASA Origins of Solar Systems grants.

REFERENCES

- Abt H.A., Wang R., Cardona O., 1991, ApJ, 367, 155
- Bate, M.R., Bonnell, I.A., Bromm, V. 2002, MNRAS, 332, L65
- Bate, M.R., Bonnell, I.A., Bromm, V. 2003, MNRAS, 277, 362
- Bate, M.R. 2009, MNRAS, 392, 590
- Bate, M.R. 2011, MNRAS, in press
- Bernasconi P.A., & Maeder A. 1996, A&A, 307, 829
- Brusa, G., et al. 2003a, Proc. SPIE 4839, 691.

- Brusa, G., et al. 2003b, Proc. SPIE 5169, 26
- Burgasser, A. et al. 2003, ApJ, 586, 512
- Burgasser, A., Reid, L.N., Siegler, N., Close, L., Allen, P., Lowerance, P., Gizis, J. (2007), Protostars and Planets V, B. Reipurth, D. Jewitt, and K. Keil (eds.), University of Arizona Press, Tucson, 951 pp., p.427-441
- Burrows, A., Hubbard, W. B., Lunine, J. I., Marley, M. S., Saumon, D. 2000, Protostars and Planets IV (Tucson: University of Arizona Press, eds Mannings, V., Boss, A.P., Russell, S. S.), p. 1339
- Bouy, H., Brandner W., Martín, E., Delfosse, X., Allard, F., & Basri, G. 2003, AJ, 126, 1526
- Bossi M., Gaspani A., Scardia M., Tadini M., 1989, A&A, 222, 117
- Chabrier, G., Baraffe, I., Allard, F., & Hauschildt, P. 2000, ApJ, 542, 464
- Close, L.M., Roddier, F.J., Roddier, C.A., Graves, J.E., Northcott, M.J., Potter, D. 1998, Proc. SPIE Vol. 3353, p. 406-416. Adaptive Optical System Technologies, D. Bonaccini, R.K. Tyson, Eds
- Close, L. M. 2000, Proc. SPIE Vol. 4007, p758-772. Adaptive Optical Systems Technology, P.L. Wizinowich, Ed.
- Close, L.M. et. al. 2002a, ApJ, 566, 1095.
- Close, L.M. et. al. 2002b, ApJ, 567, L53.
- Close, L.M., Siegler, N., Freed, M., Biller, B. 2003a ApJ, 587, 407
- Close, L.M. et al. 2003b ApJ, 598, 35.
- Close, L.M. et al. 2003c ApJ, 599, 537.
- Close, L.M. et al. 2007 ApJ, 665, 736.
- Diolaiti, E., Bendinelli, O. Bonaccini, D.; Close, L Currie, D. Parmeggiani, G. 2000, A&AS 147, 335
- Durisen, R.H., Sterzik, M.F., & Pickett, B.K. 2001, A&A, 371, 952
- Duquenois, A., Mayor, M. 1991, A&A, 248, 485
- Eggleston P., Kiseleva L., 1995, ApJ, 455, 640

- Esposito, S. et al. proc. 2011, SPIE 8149, 814902-10
- Esposito, S. et al. proc. 2010a SPIE 7736, 773609-12
- Esposito, S. et al. proc. 2010b Applied Optics, 49, issue 31, p. G174
- Fischer, D. A., Marcy, G. W. 1992, ApJ, 396, 178
- Freed, M., Close, L.M., & Siegler, N. 2003, ApJ, 584, 453
- Genzel R., Stutzki J., 1989, ARA&A 27, 41
- Graves, J.E., Northcott, M.J., Roddier, F.J., Roddier, C.A., Close, L.M. 1988, Proc. SPIE Vol. 3353, p. 34-43. Adaptive Optical System Technologies, D. Bonaccini, R.K. Tyson, Eds.
- Gizis, J.E. et al. 2003, ApJ, 120, 1085
- Hillenbrand L.A., & Carpenter J. 2000 ApJ, 540, 236
- Hillenbrand L.A., & Hartmann L.W. 1998 ApJ, 492, 540
- Hinz J.L., McCarthy D.W., Simons, D.A., Henry T.J., Kirkpatrick J.D., McGuire P.C. 2002, AJ, 123, 2027
- Hinz P.M. et al. 2010, ApJ 716 417
- Hodapp, K.-W., Hora, J. L., Hall, D. N. B., Cowie, L. L., Metzger, M., Irwin, E., Vural, K., Kozlowski, L. J., Cabelli, S. A., Chen, C. Y., Cooper, D. E., Bostrup, G. L., Bailey, R. B., Kleinhans, W. E. 1996, New Astronomy, 1, 177
- Kiseleva L.G., Eggleton P.P., Anosova J.P., 1994, MNRAS 267, 161
- Kiseleva L.G., Eggleton P.P., Orlov V.V., 1994, MNRAS 270, 936
- Kraus, S. et al. 2007, A&A 466, 649
- Kohler, R. et al. 2006, A&A 458, 461
- Lloyd-Hart M. 2000, PASP 112, 264
- McCaughrean M.J., & Stauffer J.R., 1994, AJ, 108, 1382
- McCaughrean M.J. 2000, The Formation of Binary Stars, Proceedings of IAU Symp. 200, held 10-15 April 2000, in Potsdam, Germany, Edited by Hans Zinnecker and Robert D. Mathieu, 2001, p. 169.

- McCarthy C., Zuckerman, B. (2004), AJ 127, 2871
- McCarthy D.W. et al. 1998, Proc. SPIE 3354 750
- McDonald, J. M., & Clarke, C. J. 1993, MNRAS, 262, 800
- Parker, R.J., Goodwin, S., Allison, R.J. 2011, MNRAS418, 2565
- Petr M.G., Du Foresto V., Beckwith S.V.W., Richichi A., McCaughrean M.J. 1998, ApJ, 500, 825
- Potter, D. et al. 2002a ApJ, 567, 113
- Reid, I. N., Gizis, J.E., Kirkpatrick, J.D., Koerner, D. W. 2001a, AJ, 121, 489
- Reid, I. N., Burgasser, A. J., Cruz, K. L., Kirkpatrick, J. D., Gizis, J. E. 2001b, AJ, 121, 1710
- Reipurth, B. & Clarke, C. 2001, AJ, 122, 432
- Ricci, Luca; Robberto, M.; Soderblom, D. R.; Kozhurina-Platais, V. 2007, BAAS 211, 8923
- Schertl, D., Balega, Y.Y., Preibisch, Th., & Weigelt, G. 2003, A&A, 402, 267
- Siegler, N., Close, L.M., Mamajek, E., Freed, M. 2003, ApJ, 598, 1265
- Siess L., Forestini M., Dougados C., 1997, A&A 324, 556
- Simon, M., Close, L.M., & Beck, T. 1999, AJ, 117, 1375
- Sterzik, M. F., & Durisen, R. H. 1998 A&A, 339, 95
- Stetson, P. B. 1987, PASP, 99, 191
- Wainscoat R. J., & Cowie, L.L. 1992, AJ, 103, 332.
- Weigelt G., Balega, Y., Preibisch T., Schertl D., Scholler M., Zinnecker H. 1999, A&A, 347, L15
- Wildi F., Brusa G., Riccardi A., Lloyd-Hart M., Martin H.M., L.M. Close 2003, proc. SPIE 4839, 155
- Wildi F. Brusa G., Lloyd-Hart M., Martin H.M., L.M. Close, Riccardi A. 2003b, proc SPIE 5169, 17.

Table 1. Astrometry and Narrowband Photometry of the Trapezium Cluster, Oct 16/2011, LBT

RA ^a J2000	DEC ^a J2000	X pixel ^b	Y pixel ^b	$Br\gamma$ (mag)	Phot Error	[FeII] (mag)	Phot Error	[FeII]- $Br\gamma$ Color	Comm.
15.2934	23:23.1241	1973.024	1338.378	15.326	0.016	0	0	na	no [FeII] image
15.3534	23:24.0418	1926.703	1290.952	16.102	0.012	0	0	na	no [FeII] image
15.5336	23:15.6412	1787.666	1725.089	16.035	0.015	17.715	0.024	1.68	
15.5517	23:29.5216	1773.713	1007.755	16.859	0.015	0	0	na	no [FeII] image
15.594	22:58.832	1741.035	2593.750	14.702	0.017	15.664	0.025	0.962	
15.6306	22:56.385	1712.828	2720.215	10.676	0.012	11.945	0.009	1.269	
15.7255	23:22.4347	1639.552	1374.004	11.743	0.007	12.970	0.032	1.227	
15.7673	23:9.82764	1607.314	2025.533	9.3918	0.016	9.447	0.020	0.0552	E1 single
15.7879	23:26.5168	1591.355	1163.044	12.641	0.009	13.895	0.032	1.254	$Br\gamma$ tail away from C1
15.8018	23:11.8906	1580.662	1918.921	14.409	0.041	14.971	0.033	0.562	
15.8202	23:14.2891	1566.428	1794.966	8.862	0.040	8.784	0.036	-0.078	A1 see table 2
15.8217	23:14.0972	1565.298	1804.883	10.322	0.037	10.392	0.033	0.07	A2 see table 2
15.8337	23:22.4207	1556.059	1374.727	11.521	0.005	12.827	0.031	1.306	
15.8408	23:25.5078	1550.599	1215.191	13.268	0.011	14.388	0.047	1.12	$Br\gamma$ tail away from C1
15.863	23:10.7606	1533.468	1977.318	14.411	0.023	15.485	0.041	1.074	
15.8739	23:1.89992	1524.986	2435.234	12.637	0.014	13.553	0.031	0.916	
15.9654	23:22.6589	1454.430	1362.420	16.199	0.017	17.120	0.025	0.921	
16.0635	23:24.2937	1378.699	1277.933	15.907	0.065	17.586	0.082	1.679	$Br\gamma$ tail away from C1
16.064	23:7.05258	1378.302	2168.947	12.067	0.010	11.919	0.019	-0.148	B3 see table 2
16.069	23:6.96452	1374.429	2173.498	10.025	0.011	10.845	0.017	0.82	B2 see table 2
16.0715	23:27.7444	1372.539	1099.602	15.928	0.027	17.152	0.062	1.224	$Br\gamma$ tail away from C1
16.0717	22:54.2677	1372.379	2829.663	14.591	0.015	18.480	0.049	3.889	-0.259'' binary #1B Table 3
16.0795	22:54.036	1366.341	2841.632	14.215	0.017	16.958	0.021	2.743	-binary #1A see Table 3
16.0928	23:23.0106	1356.092	1344.243	16.379	0.021	20.27	0.15	3.891	very red Brown Dwarf?
16.0942	23:6.41047	1355.015	2202.131	13.552	0.024	13.825	0.029	0.273	B4 see table 2
16.1006	23:14.1407	1350.043	1802.635	13.950	0.010	15.228	0.040	1.278	-0.187'' bin. #2A, Table 3
16.1014	23:14.2772	1349.480	1795.580	17.643	0.077	19.004	0.197	1.361	- bin. #2B, Table 3
16.1299	23:6.71895	1327.477	2186.189	8.787	0.001	8.842	0.002	0.055	B1 SB see table 2
16.1396	22:55.249	1319.930	2778.926	14.945	0.016	16.152	0.023	1.207	
16.2263	23:19.0612	1253.022	1548.345	15.072	0.014	15.861	0.089	0.789	
16.283	23:16.512	1209.290	1680.088	12.199	0.010	13.298	0.058	1.099	astrometric zeropoint ^c
16.3206	23:22.5317	1180.291	1368.992	15.185	0.029	16.261	0.029	1.076	2.115'' proj. sep. to C1
16.3241	23:25.2679	1177.537	1227.588	15.709	0.024	16.219	0.058	0.51	
16.3997	23:11.2870	1119.16	1950.11	17.12	0.2	19.196	0.070	2.076	Brown Dwarf?
16.4602	23:22.8832	1072.497	1350.827	8	1.0	8	1.0	0	C1 binary (saturated)
16.4619	23:22.8443	1071.207	1352.838	7	1.0	7	1.0	0	C2 0.046'' to C1
16.6148	23:16.0836	953.204	1702.226	12.762	0.012	14.106	0.062	1.344	
16.6529	23:28.8309	923.797	1043.453	14.928	0.011	16.050	0.058	1.122	
16.7236	23:25.1688	869.219	1232.707	11.705	0.012	11.573	0.072	-0.132	
16.7469	23:16.3777	851.247	1687.030	11.721	0.009	13.529	0.061	1.808	$Br\gamma$ tail away from C1
16.7621	23:28.0209	839.571	1085.313	13.838	0.016	14.254	0.067	0.416	
16.8258	23:25.9032	790.355	1194.754	16.951	0.045	18.094	0.075	1.143	-0.396'' bin. #3B, Table 3
16.8409	23:26.2297	778.753	1177.879	15.656	0.109	16.831	0.091	1.175	- $Br\gamma$ Bowshock Bin #3A
16.8633	23:7.03118	761.435	2170.053	15.402	0.008	16.107	0.066	0.705	
17.0595	23:33.9787	610.024	777.417	11.020	0.030	11.264	0.035	0.244	
17.1675	23:17.0013	526.70	1654.80	0.0	0.0	15.465	0.107	na	D2 1.401'' proj. sep. to D1
17.2558	23:16.5298	458.479	1679.17	0.0	0.0	8.658	0.1	na	D1 no $Br\gamma$ image

^ato calculate full RA simply prefix 5:35 to column 1 ($True_{RA} = "5 : 35 : col1"$) and for full DEC simply prefix -5: to column 2 ($True_{DEC} = " - 5 : col2"$). So for example we find θ^1 Ori C1 is at RA=5:35:16.4602 and DEC=-5:23:22.8832 (J2000).

^bthese pixels are in the $Br\gamma$ filter with a platescale of $0.019350 \pm 0.000047''/pix$. Increasing Y is due North, and increasing X is in the due West direction

^cwe used this single star (called LV3 or 163-317) as the astrometric zeropoint as it has a good position the the Hubble ACS data of Ricci et al. and is imaged in all of of our AO data. It has a location of 5:35:16.460 -5:23:22.812 J2000.

Table 2. High Resolution Observations of the θ^1 Ori B & A groups

System name	ΔH (mag)	$\Delta K'$ (mag)	Separation ($''$)	Sep. Vel. (Sep. mas/yr)	PA ($^\circ$)	PA Vel. ($^\circ$ /yr)	Telescope	epoch (m/d/y)
$B_1 B_2$	2.30 ± 0.15		$0.942 \pm 0.020''$		254.9 ± 1.0		SAO ^a	10/14/97
		1.31 ± 0.10^b	$0.942 \pm 0.020''$		254.4 ± 1.0		SAO ^a	11/03/98
		2.07 ± 0.05	$0.9388 \pm 0.0040''$		255.1 ± 1.0		GEMINI	09/19/01
	2.24 ± 0.05		$0.9375 \pm 0.0030''$		255.1 ± 1.0		MMT	01/20/03
			$0.9411 \pm 0.0023''$		254.5 ± 0.3		LBT	10/16/11
			before LBT=	-0.6 ± 1.9		0.07 ± 0.25		
			with LBT=	-0.27 ± 0.33		-0.013 ± 0.048		
			corr.=	84%; no vel. detected	corr.=	45%; no vel. detected		
$B_2 B_3$	1.00 ± 0.11		$0.114 \pm 0.05''$		204.3 ± 4.0		SAO ^a	10/14/97
		1.24 ± 0.20	$0.117 \pm 0.005''$		205.7 ± 4.0		SAO ^a	11/03/98
		1.04 ± 0.05	$0.1166 \pm 0.0040''$		207.8 ± 1.0		GEMINI	09/19/01
	0.85 ± 0.05		$0.1182 \pm 0.0030''$		209.7 ± 1.0		MMT	01/20/03
			$0.1156 \pm 0.0005''$		220.4 ± 0.3		LBT	10/16/11
			before LBT=	0.6 ± 1.0		0.93 ± 0.49		
			with LBT=	-0.10 ± 0.16		1.15 ± 0.07		
			corr.=	56%; no vel. detected		4.9 ± 0.3 km/s corr.=99.9%		
$B_1 B_4$	4.98 ± 0.10	5.05 ± 0.8	$0.609 \pm 0.008''$		298.0 ± 2.0		SAO ^c	02/07/01
		5.01 ± 0.10	$0.6126 \pm 0.0040''$		298.2 ± 1.0		GEMINI	09/19/01
			$0.6090 \pm 0.0050''$		298.4 ± 1.0		MMT	01/20/03
			$0.6157 \pm 0.003''$		300.1 ± 0.5		LBT	10/16/11
			before LBT=	-1.1 ± 1.9		0.1 ± 0.5		
			with LBT=	0.53 ± 0.25		0.18 ± 0.08		
				1.1 ± 0.5 km/s corr.=91.1%		4.13 ± 1.8 km/s corr.=99.7%		
$A_1 A_2$	1.51 ± 0.15	1.38 ± 0.10	$0.208 \pm 0.030''$		343.5 ± 5.0		Calar Alto ^d	11/15/94
		1.51 ± 0.05	$0.2215 \pm 0.005''$		353.8 ± 2.0		SAO ^a	11/03/98
		1.62 ± 0.05	$0.2051 \pm 0.0030''$		356.9 ± 1.0		GEMINI	09/19/01
			$0.1931 \pm 0.0005''$		366.5 ± 0.3		LBT	10/16/11
			before LBT=	-6.4 ± 2.7		2.13 ± 0.73		
			with LBT=	-1.4 ± 0.2		0.92 ± 0.07		
				2.9 ± 0.4 km/s corr.= 94.1%		6.6 ± 0.5 km/s corr.= 98.9%		

^aspeckle observations of Weigelt et al. (1999).

^bthese low ΔK values are possibly due to θ^1 Ori B_1 being in eclipse during the 11/03/98 observations of Weigelt et al. (1999).

^cspeckle observations of Schertl et al. (2003).

^dspeckle observations of Petr et al. (1998).

Table 3. Tight Binaries in the LBT Trapezium Field (10/16/11)

Bin. #	RA ^a J2000	DEC ^a J2000	X pixel ^b	Y pixel ^b	$\Delta Br\gamma$ (mag)	$\Delta[FeII]$ (mag)	Sep. (mas)	PA ($^{\circ}$)	Comment
1A	16.0795	22:54.036	1366.341	2841.632	0.376 ± 0.024	1.522 ± 0.053	259 ± 2	206.77 ± 0.30	B has more extinction than A A&B both very red
1B	16.0717	22:54.2677	1372.379	2829.663					
2A	16.1006	23:14.1407	1350.043	1802.635	3.693 ± 0.080	3.776 ± 0.198	136 ± 3	175.44 ± 0.30	B has strong gray extinction?
2B	16.1014	23:14.2772	1349.480	1795.580					
3A	16.8409	23:26.2297	778.753	1177.879	1.295 ± 0.064	1.263 ± 0.118	396 ± 3	325.49 ± 0.30	$Br\gamma$ Bowshock between binary?
3B	16.8258	23:25.9032	790.355	1194.754					

^aThe RA and DEC are the same format as in Table 1

^bThe X and Y location are same format as in Table 1

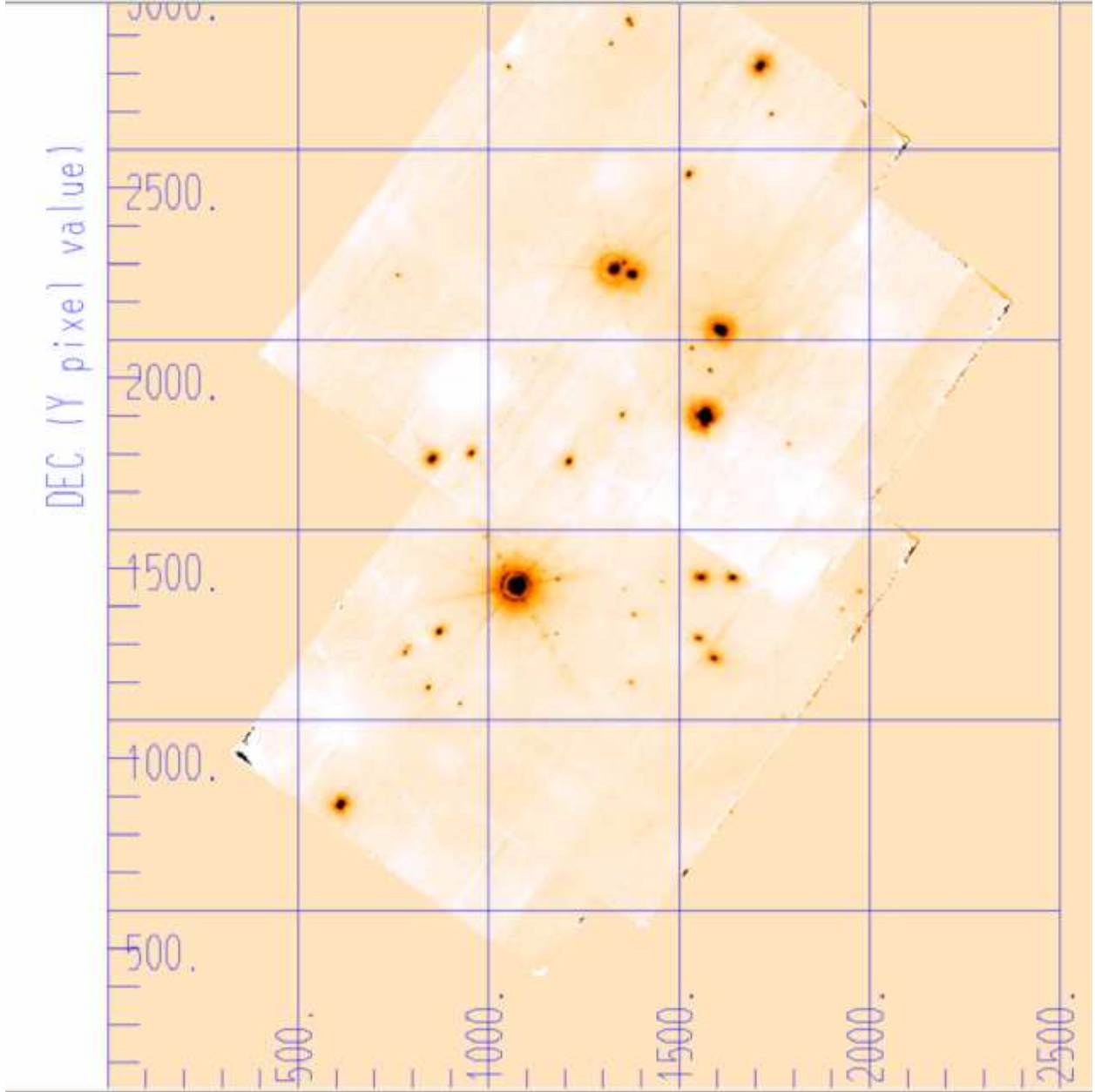


Fig. 1.— The θ^1 Ori cluster as imaged over $\sim 41 \times 53''$ FOV at LBT with the LBT AO and PISCES in $Br\gamma$. Logarithmic color scale. North is up and east is left. Note that the “rings” around the stars are limit of the ASM’s control radius $r_c = \lambda/2d \sim 0.8''$ (where the space between AO actuators maps to roughly $d \sim 0.27\text{m}$ on the LBT primary). Inside this control radius the FLAO system can “carve out” the PSF to reveal faint companions. This is the first image ever obtained which shows a field of multiple stars each with a “dark ring” in its PSF. Each pixel is 19.35 mas, see Table 1 for a complete list of the photometry and astrometry for this field. North is up, East to the left, and the X Y grid is in pixels—corresponding to the pixel values listed in Table 1. Hence this figure’s XY grid can be used to located any object from its (X,Y) coordinates in Table 1

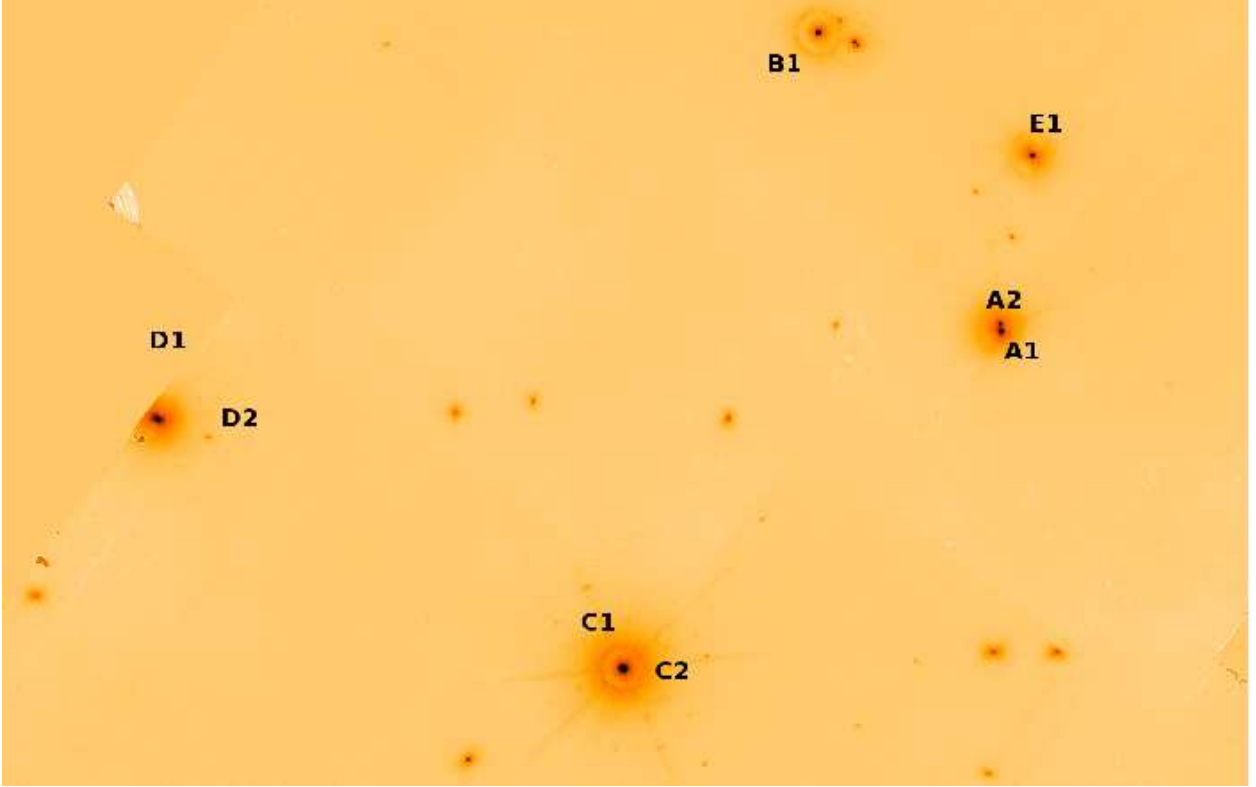


Fig. 2.— The locations and nomenclature of Close et al. (2003c) of the θ^1 Ori Trapezium stars as imaged over $\sim 35 \times 30''$ FOV at LBT with LBTAO/PISCES in [FeII]. Logarithmic color scale. North is up and east is left. Note that the object “ A_1 ” is really a spectroscopic binary (A_1A_3); where the unseen companion A_3 is separated from A_1 by 1 AU (Bossi et al. 1989). The B group is shown in more detail in Figs. 4 - 6. It is not currently clear if D2 is physically related to D1. E1 appears to be a single star. No new faint companions were discovered (at $> 5\sigma$) around any of the Trapezium stars down to brown dwarf masses ($Br\gamma < 16.0$ which converts to $K < 14$ mag) at separations $\gtrsim 0.1''$.

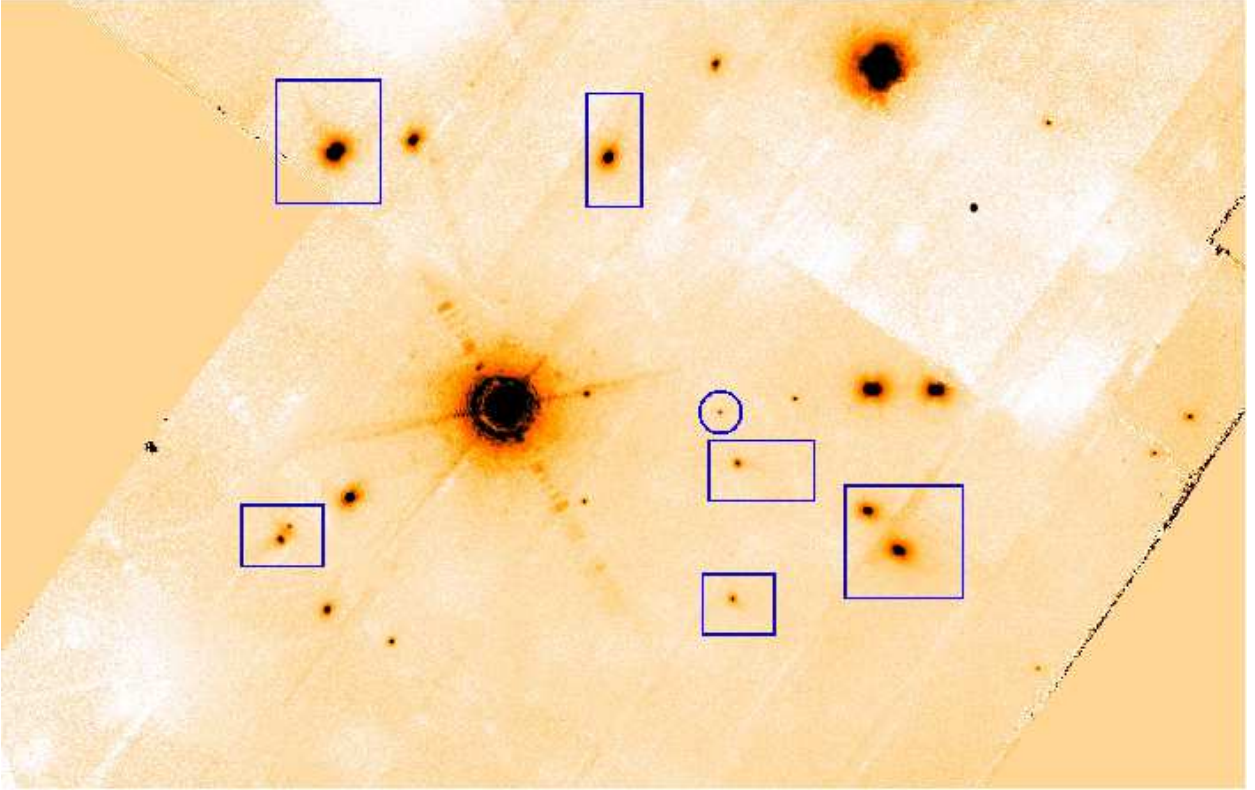


Fig. 3.— The center of θ^1 Ori C as imaged over $25 \times 20''$ FOV at LBT with LBTAO/PISCES in $Br\gamma$. Logarithmic color scale. North is up and east is left. Note the blue squares have $Br\gamma$ “tails” away from C, and the circle is around a very red $Br\gamma$ object that is much brighter at $Br\gamma$ than [FeII] or H band.

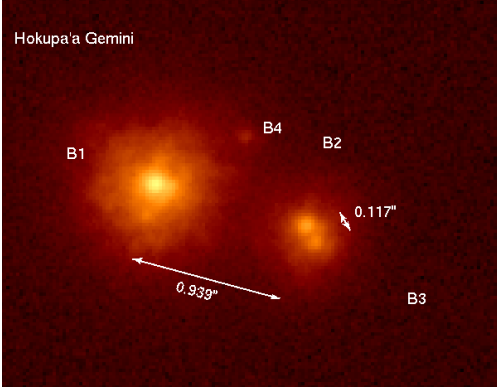


Fig. 4.— The 8m Gemini/Hokupa'a images of the θ^1 Ori B group in the K' band (09/19/01; from Close et al. (2003c)). Resolution $0.085''$. Log scale. North is up and East is left.

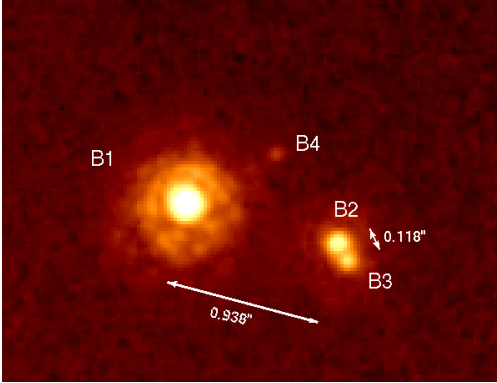


Fig. 5.— Detail of the θ^1 Ori B group as imaged at $0.077''$ (Strehl $> 20\%$) resolution (in the H band) with the MMT AO system (01/20/03) from Close et al. (2003c).

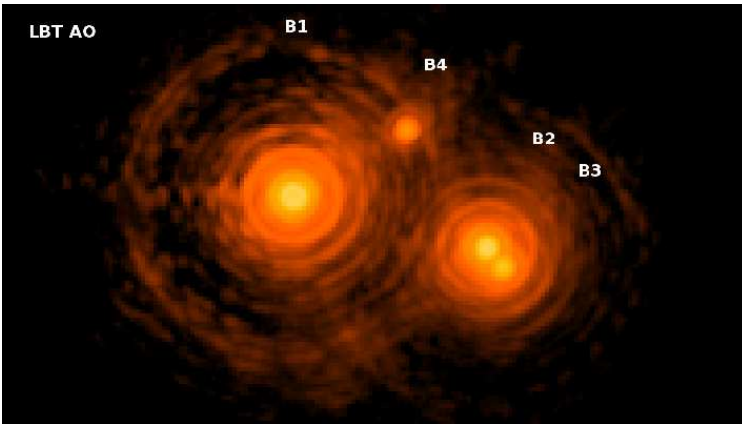


Fig. 6.— The LBT AO $Br\gamma$ images of the θ^1 Ori B group. Resolution $0.06''$. Logarithmic color scale. North is up and east is left. Strehl is $\sim 75\%$.

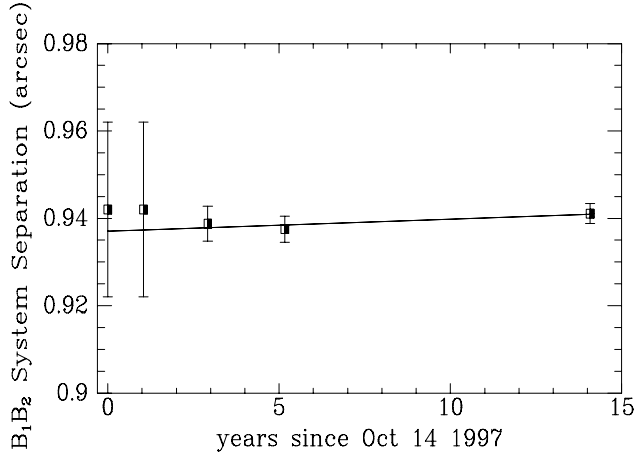


Fig. 7.— The separation between θ^1 Ori B_1 and B_2 . Note how over 15 years of observation there has been little significant relative proper motion observed (-0.27 ± 0.33 mas/yr; which is a significant correlation only at 84% level). If the group is gravitationally bound the separation change could be this low. The first 2 data points are speckle observations from the 6-m SAO telescope (Weigelt et al. 1999), the next point is from Gemini/Hokupa’a observations Close et al. (2003c) and the next data point is from the MMT AO observations Close et al. (2003c), and the last from the LBT.

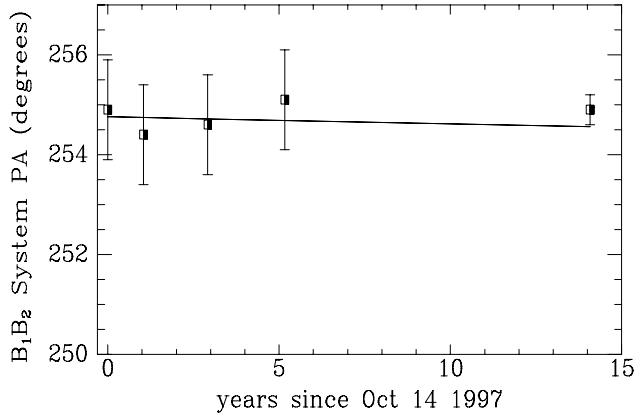


Fig. 8.— The position angle between θ^1 Ori B_1 and B_2 . Note how over 15 years of observation there has been no significant relative PA motion observed ($0.014 \pm 0.048^\circ/\text{yr}$ which is insignificantly different from zero velocity). The epochs of the data are the same as in Fig. 7.

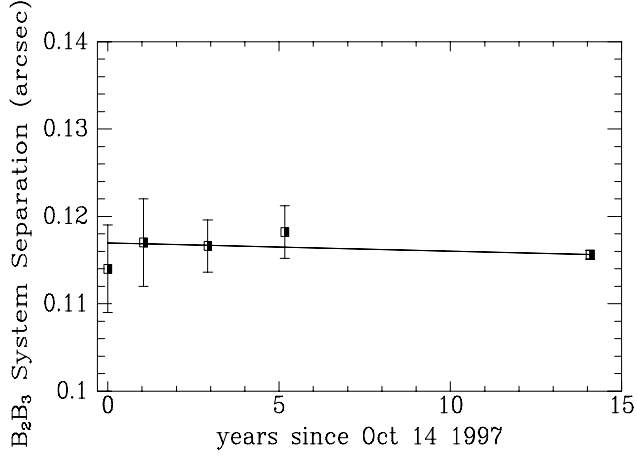


Fig. 9.— The separation between θ^1 Ori B_2 and B_3 . Note the lack of any significant relative motion (-0.095 ± 0.169 mas/yr). The rms scatter from a constant value is only 0.16 mas/yr. There appears to be very little change in the separation of the B_2B_3 system. The epochs of the data are the same as in Fig. 7.

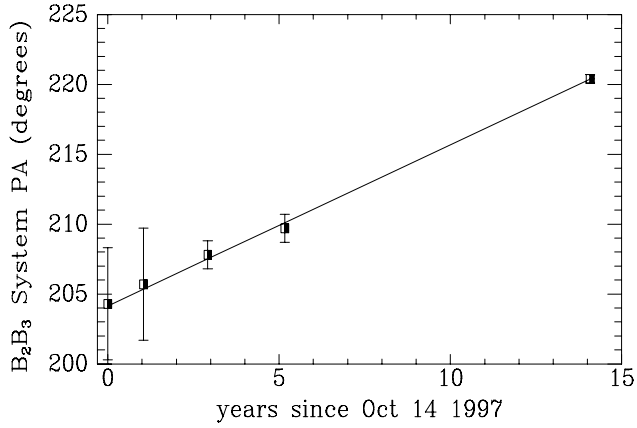


Fig. 10.— The position angle of θ^1 Ori B_2 and B_3 . Here we observe real orbital motion of B_3 moving counter-clockwise (at $1.15 \pm 0.07^\circ/\text{yr}$; correlation significant at the 99.9% level) around B_2 . This small amount of motion is consistent with the B_2B_3 system being bound. The epochs of the data are the same as in Fig. 7.

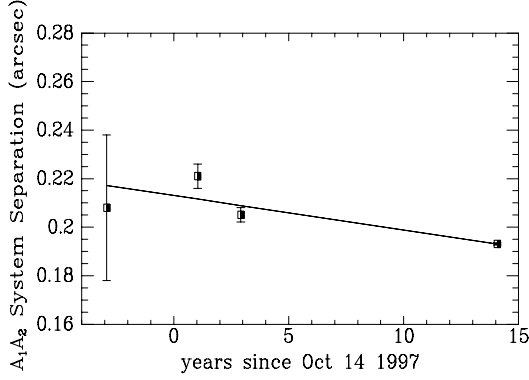


Fig. 11.— The separation between θ^1 Ori A_1 and A_2 . There is a small negative change in the orbital separation (-1.4 ± 0.22 mas/yr; correlation 94%) as A_2 moves towards A_1 . The first data point is from speckle observations at the 3.5-m Calar Alto telescope (Petr et al. 1998), the next point is from a speckle observation from the 6-m SAO telescope (Weigelt et al. 1999), the next point is from the Gemini/Hokupa’a observation of Close et al. (2003c), and the last point is from our LBT observations.

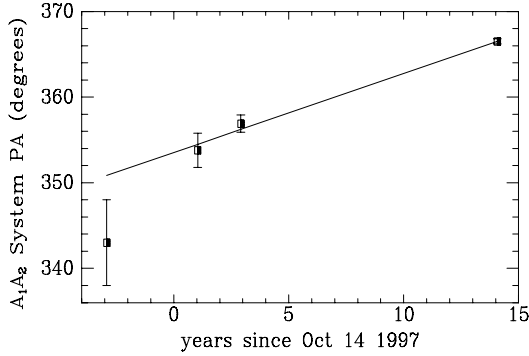


Fig. 12.— The position angle of θ^1 Ori A_1 and A_2 . There is significant (linear correlation=99%) change in the position angle as A_2 moves counter clockwise (at $0.92 \pm 0.07^\circ/\text{yr}$) around A_1 . This relatively large motion is consistent with the A_1A_2 system being bound. The first data point is from speckle observations at the 3.5-m Calar Alto telescope (Petr et al. 1998), the next point is from a speckle observation from the 6-m SAO telescope (Weigelt et al. 1999), the next point is from the Gemini/Hokupa’a observations of Close et al. (2003c) and the last point is from our LBT observations.

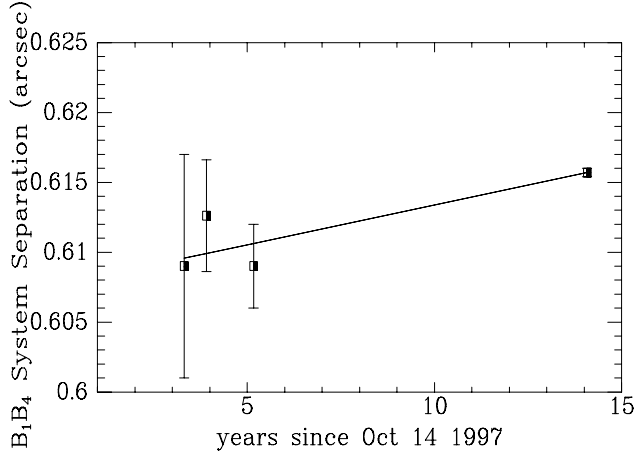


Fig. 13.— The separation between θ^1 Ori B_1 and B_4 . Note how over 12 years of observation there been only now significant relative proper motion observed (0.53 ± 0.24 mas/yr; correlation 91%). If the low mass star B_4 is gravitationally bound to the B group the B_1B_4 separation should be roughly changing at a rate of this order. The first data point is an speckle observation from the 6-m SAO telescope (Schertl et al. 2003), the next is from the Gemini/Hokupa’a observation Close et al. (2003c) and the next data point is from the MMT AO observation Close et al. (2003c) and the last is from the LBT.

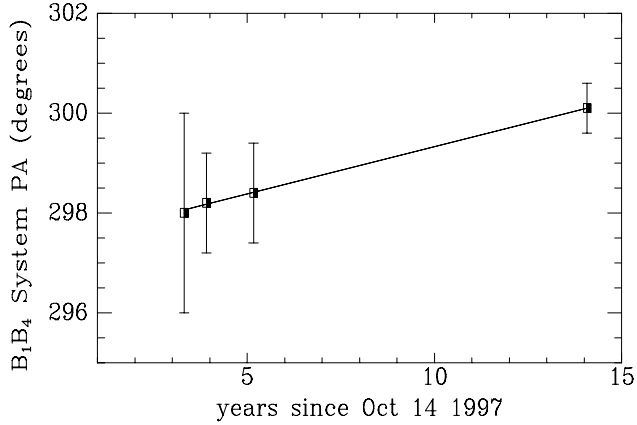


Fig. 14.— The position angle between θ^1 Ori B_1 and B_4 . Note how over 12 years of observation there has been only now a detectable significant relative proper motion observed ($0.18 \pm 0.08^\circ$ /yr; correlation 99.7%). The sources of the data is the same as in Fig. 13.